

Stabilities and Nature of the Attractive Interactions in HeBeO, NeBeO, and ArBeO and a Comparison with Analogues NGLiF, NGBN, and NGLiH (NG = He, Ar). A Theoretical Investigation

Gernot Frenking,^{*,1a} Wolfram Koch,^{†,1b} Jürgen Gauss,^{1c} and Dieter Cremer^{*,1c}

Contribution from the Molecular Research Institute, 701 Welch Road, Palo Alto, California 94304, the Institut für Organische Chemie, Technische Universität Berlin, Strasse des 17. Juni 135, D-1000 Berlin 12, West Germany, and the Institut für Organische Chemie, Universität Köln, Greinstrasse 4, D-5000 Köln 41, West Germany.
Received February 3, 1988

Abstract: Results of ab initio calculations are reported for HeBeO (1), NeBeO (2), ArBeO (3), HeLiF (4), ArLiF (5), HeBN (6), ArBN (7), and HeLiH (8). At the MP2/6-31G(d,p) level, the NGBeO structures 1-3 are predicted with rather short NG-Be distances, while for 4-8 significantly longer NG-X distances are found. Dissociation into the respective noble-gas atom NG and BeO is calculated at the MP4(SDTQ)/6-311G(2df,2pd) level corrected by zero-point energies and basis set superposition error to be endothermic by 3.1 kcal/mol for 1, 2.2 kcal/mol for 2, and 7.0 kcal/mol for 3. For 4-8, dissociation energies $D_0 \leq 0.1$ kcal/mol are predicted. Interactions of NG with BeO in 1-3 are investigated by analysis of the one-electron density distribution and compared with interactions between NG and Be in diatomic cations HeBeⁿ⁺, NeBeⁿ⁺, and ArBeⁿ⁺ ($n = 1, 2$). It is concluded that the stability of NGBeO can be explained on the basis of relatively strong charge-induced dipole interactions typical of van der Waals complexes. Vibrational frequencies and infrared intensities are reported for 1-3 to aid experimental identification. For HeBeO and HeBN CASSCF geometry optimizations have additionally been performed using the 6-31G(d,p) basis set and a full-valence active space.

1. Introduction

Bartlett,² 26 years ago, synthesized the first neutral compound containing a noble-gas element by reacting xenon with platinum hexafluoride, PtF₆. He had recognized that the first ionization energy of xenon was small enough to allow the formation of chemical bonds, a result which prior to Bartlett's discovery was believed to be impossible. In the following years noble-gas chemistry developed rapidly, and already in 1963 the first monograph on noble-gas compounds was published.³ In 1970 an entire volume of Gmelin's *Handbuch der Anorganischen Chemie* was devoted to this class of compounds.⁴ A 1978 bibliography contains 1192 theoretical and experimental references on this subject.⁵ Noble-gas chemistry is now a standard part of inorganic textbooks,⁶ and many ionic and covalent compounds containing noble-gas elements have been synthesized and studied.

However, the key to noble-gas chemistry, i.e., the ionization energy (IE) of the noble gas (NG), only unlocked the door to the chemistry of Kr, Xe, and Rn. The stability of the noble-gas compounds is mainly determined by (i) the IE value of NG and (ii) the electronegativity χ of the binding partner A. Stability toward dissociation decreases rapidly with increasing IE(NG) and decreasing electronegativity χ of A. This explains why noble-gas chemistry to a large extent is synonymous with xenon chemistry, and that the most stable Xe bonds are formed with highly electronegative elements such as fluorine, oxygen, nitrogen, and chlorine. The high IE values⁷ of He (24.587 eV), Ne (21.564 eV), and Ar (15.759 eV) prevent the formation of stable neutral compounds with highly electronegative binding partners. From the knowledge gained so far it has been concluded that the threshold of true chemical reactivity is reached with krypton.⁶ However, it has recently been suggested⁸ that ArF⁺ may form a stable salt with a suitable YF₆⁻ anion, because ArF⁺ is theoretically predicted to have a $1^2\Sigma^+$ ground state with a binding energy of ca. 50 kcal/mol.

Electronegative elements attract electronic charge from other atoms via Coulombic forces. A different mechanism can be visualized when a group or atom provides empty orbitals and acts as a Lewis acid. Then, the noble gas as a Lewis base may donate

electronic charge possibly forming a semipolar bond. Such an approach has experimentally been tested as early as 1935 for the reaction of argon with BF₃.⁹ Early ab initio investigations at the LCAO-SCF level calculated the interaction of He, Ne, and Ar with electropositive atoms and groups such as Li, Be, Na, LiH, BeH₂, BeH, and other species.^{5,10,11} HeLiH was predicted to be bound by 0.08 eV (1.8 kcal/mol),^{10a} and the existence of rare-gas complexes with light-weight electron-deficient hydrides was stated to be a distinct possibility.¹⁰

Weakly bound neutral complexes of the noble-gas elements, including He, Ne, and Ar, have long been known.^{3a,5} With the advent of the supersonic nozzle,¹² detailed information concerning the structures, stabilities, and spectroscopic properties are known now for molecules such as NGNO, NGHf, NGHCl (NG = Ne, Ar), and others.^{13,14} However, the structural data obtained from

(1) (a) Molecular Research Institute. (b) IBM Almaden Research Center. (c) Universität Köln.

(2) Bartlett, N. *Proc. Chem. Soc.* 1962, 218.

(3) (a) Hyman, H. H., Ed. *Noble-Gas Compounds*; The University of Chicago Press: Chicago, 1963. (b) Bartlett, N. *The Chemistry of the Noble Gases*; Elsevier: Amsterdam, 1971. (c) Holloway, J. H. *Chem. Brit.* 1987, 65B. (d) Holloway, J. H. *Noble Gas Chemistry*; Methuen: London, 1968.

(4) *Gmelin's Handbuch der Anorganischen Chemie*; Verlag Chemie: Weinheim, 1970; Sektion 1.

(5) Hawkins, D. T.; Falconer, W. E.; Bartlett, N. *Noble-Gas Chemistry. A Bibliography: 1962-1976*; IFI/Plenum: New York, 1978.

(6) Cotton, F. A.; Wilkinson, G. *Advanced Inorganic Chemistry*; Wiley: New York, 1980.

(7) Moore, C. E. *Analyses of Optical Spectra*, NSRDS-NBS 34; National Bureau of Standards: Washington, D.C.

(8) (a) Frenking, G.; Koch, W.; Deakne, C.; Liebman, J. F.; Bartlett, N. *J. Am. Chem. Soc.*, in press. (b) Frenking, G.; Koch, W.; Gauss, J.; Cremer, D.; Liebman, J. F. *J. Phys. Chem.*, submitted for publication.

(9) Booth, H. S.; Willson, K. S. *J. Am. Chem. Soc.* 1935, 57, 2273, 2280.

(10) (a) Kaufman, J. J.; Sachs, L. M. *J. Chem. Phys.* 1969, 51, 2992. (b) Kaufman, J. J.; Sachs, L. M. *J. Chem. Phys.* 1970, 52, 3534. (c) Catlow, G. W.; McDowell, M. R. C.; Kaufman, J. J.; Sachs, L. M.; Chang, E. S. *J. Phys. B* 1970, 3, 833. (d) Kaufman, J. J. *J. Chem. Phys.* 1973, 58, 4880.

(11) Krauss, M.; Maldonado, P.; Wahl, A. C. *J. Chem. Phys.* 1971, 54, 4944. (b) Riemenschneider, B. R.; Kestner, N. R. *Chem. Phys.* 1974, 3, 193. (c) Schneiderman, S. B.; Michels, H. H. *J. Chem. Phys.* 1965, 42, 3706.

(12) Levy, D. H. *Annu. Rev. Phys. Chem.* 1980, 31, 197.

(13) (a) Miller, J. C.; Cheng, W. C. *J. Phys. Chem.* 1985, 89, 1647. (b) Miller, J. C. *J. Chem. Phys.* 1987, 86, 3166. (c) Sato, K.; Achiba, Y.; Kimura, K. *J. Chem. Phys.* 1984, 81, 57. (d) Sato, K.; Achiba, Y.; Nakamura, H.; Kimura, K. *J. Chem. Phys.* 1986, 85, 1418.

[†] Present address: IBM Wissenschaftliches Zentrum, Tiergartenstrasse 15, D-6900 Heidelberg, West Germany.

experimental results clearly indicate that these species are van der Waals complexes which are bound only by very weak (<1.0 kcal/mol) long-range Coulombic interaction between induced and/or permanent dipole moments.^{13,14} Thus, a neutral compound containing chemically bound He, Ne, or Ar has not been observed.

Recently we reported theoretical studies of doubly charged cations containing helium which showed that He may form covalent bonds with binding energies of more than 80 kcal/mol.^{15,16} Also in singly charged cations, helium may be bound with dissociation energies of >20 kcal/mol.¹⁶ Investigation of the bonding features of the helium bonds with the aid of the one-electron density distribution revealed that it is the electronic structure of the electron acceptor, rather than its (positive) charge, that determines the bond strength of the helium bond. Only if a binding partner provides low-lying empty orbitals does the He atom donate electrons and form a semipolar, covalent bond.¹⁶ The model of donor-acceptor interactions proved also to be very powerful in the explanation of the trends in bond lengths and binding energies of singly and doubly charged first-row diatomic cations HeX^{n+} ($X = \text{Li-Ne}$; $n = 1, 2$),¹⁷ which are very different compared to isoelectronic hydrogen compounds.¹⁸ A similar approach has successfully been used to analyze the attractive interactions in neon and argon cations NeX^+ and ArX^+ ($X = \text{Li-Ne}$).^{8b} A systematic search for a possible *neutral* acceptor which might attract helium was finally successful: HeBeO (**1**) was calculated to be stable in its ground state with a dissociation energy of ca. 3 kcal/mol.^{16,19}

In this paper, we report a detailed study on the stabilities, bonding features, and IR spectra of **1** and the neon and argon analogues NeBeO (**2**) and ArBeO (**3**) at various levels of theory. The properties of **1-3** are compared with those of the isoelectronic HeLiF (**4**), ArLiF (**5**), HeBN (**6**) and ArBN (**7**). We also report our theoretical results on HeLiH (**8**), which has previously^{10a} been predicted to be a stable molecule. In our investigation we have been concerned with the following questions.

(a) How different and how reliable are the theoretical results at various levels of theory? How important are corrections with regard to basis-set superposition error?

(b) What is the nature of the He-Be interactions in HeBeO ? Should HeBeO be classified as a (covalently bonded) chemical compound or as a van der Waals complex?

(c) What are the differences among the noble-gas interactions of HeBeO , NeBeO , and ArBeO ? Do NG-Be interactions become stronger when going from He to Ne or Ar?

(d) How do the NGBeO structures compare with isoelectronic NGLiF and NGBN ? What determines the differences in the interactions between NG and BeO, NG and LiF, and NG and BN? Is HeLiH a stable molecule as previously^{10b} suggested?

(e) How can an identification of NGBeO with the aid of IR spectroscopy be facilitated?

(f) What is the chemical relevance of our theoretical results?

We will answer these questions by analyzing the theoretically obtained equilibrium geometries, energies, vibrational frequencies, IR intensities, and the one-electron density distribution using

techniques that have been proven very useful in our previous study on helium chemistry¹⁶ and dications.²⁰

2. Quantum Chemical Methods

A major part of our theoretical results has been obtained using the CRAY version of GAUSSIAN 82.²¹ As a standard, molecular geometries were optimized both at the Hartree-Fock (HF) and the second-order Møller-Plesset (MP2) perturbation²² level employing the 6-31G(d,p) basis set. These levels of theory are denoted by HF/6-31G(d,p) and MP2/6-31G(d,p). Geometry optimizations were carried out using analytical gradients which are a standard part of GAUSSIAN 82.²¹ For reasons which are outlined below, the geometries of BN, HeBN, and ArBN have additionally been calculated at MP3/6-31G(d,p) using the Fletcher-Powell optimization algorithm.²³ Vibrational frequencies and zero-point energies (ZPE) are determined at HF/6-31G(d,p) and MP2/6-31G(d,p). The ZPE values have been scaled uniformly by a factor of 0.87 and 0.93 for the two levels of theory.²⁴ The scaling accounts for basis set and correlation errors and errors due to the harmonic approximation in the calculation of the vibrational frequencies. However, these scaling factors are not appropriate when multiple bonds between first-row atoms are involved²⁴ such as in BeO and BN. While this does not affect ZPE corrections for the dissociation energies significantly, since similar errors are made for products and reactants, scaled frequencies may still differ significantly from experimental values. Therefore, the unscaled values are used as a basis for the discussion of the vibrational spectra. All reported structures are characterized as minima on the potential energy hypersurfaces by having only positive eigenvalues of the diagonalized force-constant matrix.

The geometries of HeBeO , HeBN , BeO , and BN have also been optimized using full-valence CASSCF wave functions with a 6-31G(d,p) basis set. The active space was 8 electrons in 8 orbitals for BeO and BN, which gives 1764 configurations, and the active space for HeBeO and HeBN consists of 10 electrons in 9 orbitals, which gives 5292 configurations. For the CASSCF studies, the program GAMESS²⁵ was employed which allows geometry optimizations using analytical first derivatives. In case of HeBN, the optimization was stopped at a He-B distance of 3.05 Å. Although the gradient norm was rather small (0.0005), the calculated step size for the He-B distance was still large, indicating a further increase in the interatomic distance.

Using the geometries obtained at the correlated level, i.e., MP3/6-31G(d,p) for BN, HeBN, and ArBN, and MP2/6-31G(d,p) for the other molecules, single-point energies are calculated with a larger basis set and fourth-order Møller-Plesset perturbation theory.²² For the argon compounds, the theoretical level is MP4(SDTQ)/6-311G(d,p) and for the helium and neon species it is MP4(SDTQ)/6-311G(2df,2pd). The basis-set superposition errors (BSSE) for the theoretically predicted dissociation energies are determined at all levels of theory using the counterpoise method;²⁶ i.e., the energies of the noble-gas atoms and of the binding fragments are calculated with the complete basis set of the respective noble-gas compound in its equilibrium geometry.

(14) (a) Harris, S. J.; Novick, S. E.; Klemperer, W. *J. Chem. Phys.* **1974**, *60*, 3208. (b) Dixon, T. A.; Joyner, C. H.; Baiocchi, F. A.; Klemperer, W. *J. Chem. Phys.* **1981**, *74*, 6539. (c) Keenan, M. R.; Buxton, L. W.; Balle, T. J.; Flygare, W. H. *J. Chem. Phys.* **1981**, *74*, 2133. (d) Hutson, J. M.; Howard, B. J. *Mol. Phys.* **1982**, *45*, 791. (e) Novick, S. E.; Davies, P.; Harris, S. J.; Klemperer, W. *J. Chem. Phys.* **1973**, *59*, 2273. (f) Hutson, J. M.; Howard, B. J. *Mol. Phys.* **1982**, *45*, 769. (g) Harris, S. J.; Novick, S. E.; Klemperer, W.; Falconer, W. E. *J. Chem. Phys.* **1974**, *61*, 193.

(15) (a) Koch, W.; Frenking, G. *Int. J. Mass Spectrom. Ion Processes* **1986**, *74*, 133. (b) Koch, W.; Frenking, G. *J. Chem. Soc., Chem. Commun.* **1986**, 1095.

(16) Koch, W.; Frenking, G.; Gauss, J.; Cremer, D.; Collins, J. R. *J. Am. Chem. Soc.* **1987**, *109*, 5917.

(17) Frenking, G.; Koch, W.; Gauss, J.; Cremer, D.; Liebman, J. F., *J. Phys. Chem.*, in press.

(18) A systematic comparison of isoelectronic hydrogen and helium(+) compounds is presented by the following: Frenking, G.; Koch, W.; Liebman, J. F. In *Molecular Structure and Energetics*; Greenberg, A., Liebman, J. F., Eds.; VCH Publishers: Deerfield, FL; Vol. 8, in press.

(19) Koch, W.; Collins, J. R.; Frenking, G. *Chem. Phys. Lett.* **1986**, *132*, 330.

(20) Koch, W.; Frenking, G.; Gauss, J.; Cremer, D. *J. Am. Chem. Soc.* **1986**, *108*, 5808.

(21) Binkley, J. S.; Frisch, M. J.; DeFrees, D. J.; Raghavachari, K.; Whiteside, R. A.; Schlegel, H. B.; Fluder, E. M.; Pople, J. A. GAUSSIAN 82, Version K, Carnegie-Mellon University: Pittsburgh, PA.

(22) Møller, C.; Plesset, M. S. *Phys. Rev.* **1934**, *46*, 618. (b) Binkley, J. S.; Pople, J. A. *Int. J. Quantum Chem.* **1975**, *9S*, 229.

(23) (a) Davidon, W. C. *Comput. J.* **1968**, *10*, 406. (b) Fletcher, R.; Powell, M. J. D. *Comput. J.* **1963**, *6*, 163.

(24) Hout, R. F.; Levi, B. A.; Hehre, W. J. *J. Comput. Chem.* **1982**, *3*, 234.

(25) Dupuis, M.; Spangler, D.; Wendoloski, J. *National Resource for Computations in Chemistry*, Software Catalog, Vol. 1, Program QG01, 1980. Revised version prepared for San Diego Super Computer Center by Schmidt, M.; Elbert, S., 1986.

(26) (a) Boys, S. F.; Bernardi, F. *Mol. Phys.* **1970**, *19*, 553. (b) Van Lenthe, J. H.; Van Duijneveldt-Van De Rijdt, J. G. C. M.; Van Duijneveldt, F. B. *Ab Initio Methods in Quantum Chemistry*; Lawley, K. P., Ed.; Wiley: New York, 1987. (c) Chalasinski, G.; Funk, D. J.; Simons, J.; Breckenridge, W. H. *J. Chem. Phys.* **1987**, *87*, 3569.

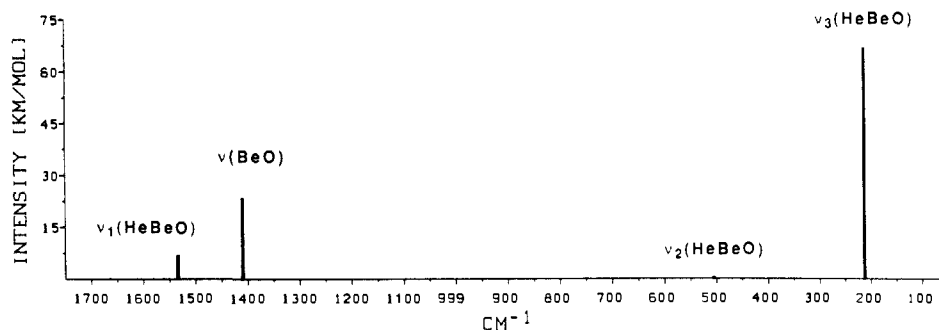


Figure 1. Theoretically predicted infrared spectra of HeBeO (1) and BeO at MP4(SDQ)/6-311G(2d,2p).

The use of the full counterpoise method for weakly bound compounds has recently been justified.^{26b,c}

As discussed below, the noble-gas structures HeBeO, NeBeO, and ArBeO are predicted by our results to be stable toward dissociation into NG and BeO. To facilitate experimental identification of the three species, we have calculated vibrational frequencies and infrared intensities of 1–3 using analytical derivatives of the total energies with respect to the nuclear coordinates and to the electric field at MP2/6-31G(d,p).^{21,27} Recently, analytical gradients to calculate geometries at the MP3 and MP4(SDQ) level of theory have been developed and coded for the program COLOGNE 85.²⁷ These procedures are employed here for 1–3.

The analysis of the total electron density distribution $\rho(r)$ is based on the investigation of its critical (stationary) points r_s , which are the sources and sinks of the gradient paths (trajectories) of the gradient vector field $\nabla\rho(r)$.²⁸ Of particular interest are the properties of $\rho(r)$ at the critical point r_b in the region between two bonded atoms A and B. The point r_b corresponds to a minimum of $\rho(r)$ along a path of maximum electron density (MED path) connecting the two atoms in question; i.e., $\rho(r_b) = \rho_b$ is a saddle point of $\rho(r)$ in three dimensions.²⁹ The MED path can be considered as an image of the chemical bond. However, MED paths are also found in the case of van der Waals interactions between atoms or molecules with closed shells.³⁰ In order to distinguish between interactions leading to covalent bonding and those in a van der Waals complex, an analysis of the electron density distribution $H(r)$ ^{30,31} was suggested. For all structures investigated so far, $H(r_b) = H_b$ has been found to be negative (positive) in case of covalent bonding (closed-shell interactions).^{30–35} This observation has been used to set up two conditions for covalent bonding, namely, (i) the existence of a critical point r_b and its associated MED path linking the nuclei in question (necessary condition) and (ii) $H_b < 0$ indicating that the accumulation of negative charge in the internuclear region is stabilizing (sufficient condition). If (ii) is fulfilled, the MED path can be called a "bond path" and r_b the "bond critical point".

Information about bonding can be substantiated by analyzing the Laplace field of $\rho(r)$, $-\nabla^2\rho(r)$, which is indicative of con-

centration ($\nabla^2\rho(r) < 0$) and depletion ($\nabla^2\rho(r) > 0$) of negative charge.^{31,36} The Laplace distribution of an isolated atom reflects the shell structure of the electrons in the atom. Upon formation of a molecule or a van der Waals complex, distortions in the Laplace distribution are indicative of the nature of the atom–atom interactions and concomitant changes in the electronic structure. The analysis of $\rho(r)$ and its associated Laplace field has led to useful descriptions of bonding in hydrocarbons,²⁹ small rings,^{32,33} π complexes,³² Be compounds,³⁴ Si compounds,³⁵ charged species,²⁰ and He–C compounds.¹⁶

3. Structures and Stabilities

The calculated energies at various levels of theory for 1–8 and the corresponding dissociation products are listed in Table I. Table II shows the optimized interatomic distances. Experimental bond lengths³⁷ are also listed in Table II. The calculated dissociation energies D_0 for 1–8 are shown in Table III.

HeBeO (1). At all levels of theory employed in our study, 1 is predicted to be stable toward dissociation into He and BeO in its $^1\Sigma^+(4\pi)$ ground state. The predicted dissociation energies D_0 corrected by the BSSE vary between 2.3 and 3.7 kcal/mol (Table III). At MP4(SDTQ)/6-311G(2df,2pd)//MP2/6-31G(d,p) + ZPE + BSSE, the stabilization energy is calculated as 2.6 kcal/mol.³⁸ The CASSCF value of 3.5 kcal/mol for D_e is in the same range as the results obtained via perturbation theory. The data for 1 shown in Table III indicate that the calculated dissociation energies become lower when correlation corrections are improved, i.e., when going from HF to MP2 and MP4. However, this result is only achieved when the error due to BSSE is accounted for. The data in Table I show that the BSSE values also increase with the sequence HF < MP2 < MP4. On the other hand, the dissociation energy increases when the basis set is improved. The HF and MP2 values for D_0 obtained with the 6-311G(2df,2pd) basis set are larger than the respective results obtained with the 6-31G(d,p) basis set.

Besides the optimizations at HF/6-31G(d,p) and MP2/6-31G(d,p), the geometry of 1 has been calculated at several levels of theory using analytical gradients²⁷ in order to study the influence of the theoretical level on the predicted bond lengths. Table IV shows the results for 1 and BeO. Since the experimentally determined equilibrium distance of BeO is known,³⁷ the reliability of theoretical results can be tested. Table IV shows that the HF/6-31G(d,p) value of the Be–O distance is too short by 0.026 Å, while the corresponding MP2/6-31(d,p) value is too long by 0.025 Å. It is gratifying that at the CAS/6-31G(d,p) and MP4(SDQ)/6-311G(2d,2p) levels of theory, the calculated r_e value for BeO (1.336 and 1.333 Å, Table IV) is close to the experimental value. At all correlated levels of theory shown in Table IV, the

(27) Gauss, J.; Cremer, D. *Chem. Phys. Lett.* **1987**, *138*, 131.

(28) Bader, R. F. W.; Nguyen-Dang, T. T.; Tal, Y. *Rep. Prog. Phys.* **1981**, *44*, 893.

(29) (a) Bader, R. F. W.; Slee, T. S.; Cremer, D.; Kraka, E. *J. Am. Chem. Soc.* **1983**, *105*, 5061. (b) Cremer, D.; Kraka, E.; Slee, T. S.; Bader, R. F. W.; Lau, C. D. H.; Nguyen-Dang, T. T.; MacDougall, P. J. *J. Am. Chem. Soc.* **1983**, *105*, 5069.

(30) (a) Cremer, D.; Kraka, E. *Croat. Chem. Acta* **1985**, *57*, 1265. (b) Cremer, D. In *Modelling of Structure and Properties of Molecules*; Maksic, Z. B., Ed.; Ellis Horwood: Chichester, 1987; p 125.

(31) Cremer, D.; Kraka, E. *Angew. Chem.* **1984**, *96*, 612; *Angew. Chem., Int. Ed. Engl.* **1984**, *23*, 627.

(32) (a) Cremer, D.; Kraka, E. *J. Am. Chem. Soc.* **1985**, *107*, 3800, 3811.

(b) Cremer, D.; Kraka, E. In *Molecular Structure and Energetics*; Greenberg, A., Liebman, J., Eds.; VCH Publishers: Deerfield, FL; Vol. 7, in press.

(33) (a) Cremer, D.; Gauss, J. *J. Am. Chem. Soc.* **1986**, *108*, 7467. (b) Gauss, J.; Cremer, D., to be published.

(34) Koch, W.; Frenking, G.; Gauss, J.; Cremer, D.; Sawaryn, A.; Schleyer, P. V. R. *J. Am. Chem. Soc.* **1986**, *108*, 5732.

(35) Cremer, D.; Gauss, J.; Kraka, E.; *THEOCHEM*, special issue in honor of L. Pauling, in press.

(36) (a) Bader, R. F. W.; MacDougall, P. J.; Lau, C. D. H. *J. Am. Chem. Soc.* **1984**, *106*, 1594. (b) Bader, R. F. W.; Essen, H. *J. Chem. Phys.* **1984**, *80*, 1943.

(37) Huber, K. P.; Hertzberg, G. *Constants of Diatomic Molecules*; Van Nostrand Reinhold: New York, 1979.

(38) In ref 16, a dissociation energy of 3.0 kcal/mol has been reported for HeBeO at the MP4(SDTQ)/6-311G(2df,2pd)//MP2/6-31G(d,p) + ZPE + BSSE level. The value reported here (2.6 kcal/mol) is slightly different, because in our earlier study the BSSE correction was carried out only for the energy calculation of He in the full HeBeO basis set, but not for BeO.

Table I. Calculated Total Energies (E_{tot} , in hartrees), Basis-Set Superposition Errors (BSSE, in kcal/mol), and Zero-Point Vibrational Energies (ZPE, in kcal/mol)

		HF/6-31G(d,p)// HF/6-31G(d,p)		MP2/6-31G(d,p)// MP2/6-31G(d,p)			MP3/6-31G(d,p)// MP3/6-31G(d,p)		6-311G(2df,2pd)//MP2/6-31G(d,p) ^j				CAS/ 6-31G(d,p)// CAS/ 6-31G(d,p)			
		E_{tot}	BSSE	ZPE	E_{tot}	BSSE	ZPE	E_{tot}	BSSE	HF/		MP2/		MP4(SDTQ)/		E_{tot}
										E_{tot}	BSSE	E_{tot}	BSSE	E_{tot}	BSSE	
HeBeO	1 $^1\Sigma^+$	-92.2710	0.4	3.2	-92.5428	1.0	3.3			-92.3060	0.2	-92.6359	0.5	-92.6575	0.6	-92.4252
NeBeO	2 $^1\Sigma^+$	-217.8966	2.9	2.9	-218.2980	5.1	2.9			-217.9717	2.7	-218.5312	5.5	-218.5539	5.8	
ArBeO	3 $^1\Sigma^+$	-616.1971	0.9	2.9	-616.5952	4.1	2.9			-616.2514 ^a	1.2	-616.6644 ^a	5.0	-616.6929 ^a	5.2	
HeLiF	4 $^1\Sigma^+$	-109.7905	0.4	1.5	-110.0117	0.6	1.7			-109.8362	0.1	-110.1420	0.2	-110.1559	0.2	
ArLiF	5 $^1\Sigma^+$	-633.7104	0.7	1.5	-634.0558	3.2	1.8			-633.7764 ^a	0.5	-634.1521 ^a	2.4	-634.1710 ^a	2.7	
HeBN	6 $^1\Sigma^+$	-81.7513	0.3	4.5	-82.0703	0.1	nc ^f	-82.0290	0.7	-81.7807	0.2	-82.1142	1.0	-82.1431	1.0	-81.9437 ^k
ArBN	7 $^1\Sigma^+$	-605.6818	0.4	3.8	-606.1033	3.7	3.0	-606.0857	3.7	-605.7335 ^a	0.5	-606.1587 ^a	4.3	-606.1938 ^a	4.5	
HeLiH	8 $^1\Sigma^+$	-10.8376	0.5	2.1	-10.8842	0.7	2.3			-10.8466	0.2	-10.9055	0.2	-10.9189	0.2	
He	1S	-2.8552	0.3 ^b		-2.8806	0.6 ^b		-2.8861	0.5	-2.8599	0.1 ^b	-2.8915	0.2 ^b	-2.8972	0.2 ^b	-2.8552
			0.3 ^c			0.5 ^c					0.1 ^c		0.1 ^c		0.1 ^c	
			0.3 ^e			0.5 ^e					0.1 ^e		0.1 ^e		0.1 ^e	
			0.2 ^f			0.1 ^f					0.1 ^f		0.3 ^f		0.3 ^f	
Ne	1S	-128.4744	2.6		-128.6262	4.5				-128.5226	2.6	-128.7797	5.3	-128.7867	5.5	
Ar	1S	-526.7737	0.3 ^e		-526.9200	3.1 ^e		-526.9231	3.3	-526.8066 ^a	0.2 ^e	-526.9539 ^a	3.6 ^e	-526.9673 ^a	3.9 ^e	
			3.0 ^f			2.6 ^f					0.2 ^f		1.9 ^f		2.1 ^f	
			0.3 ^h			3.1 ^h					0.2 ^h		3.8 ^h		4.1 ^h	
BeO	$^1\Sigma^+$	-89.4091	0.1 ^b	2.2	-89.6547	0.4 ^b	1.9			-89.4376	0.1 ^b	-89.7361	0.3 ^b	-89.7529	0.4 ^b	-89.5644
			0.3 ^d			0.6 ^d				-89.4291 ^a	0.1 ^d	-89.6885 ^a	0.2 ^d	-89.7046 ^a	0.3 ^d	
			0.6 ^e			1.0 ^e					1.0 ^e		1.4 ^e		1.3 ^e	
LiF	$^1\Sigma^+$	-106.9342	0.1 ^c	1.3	-107.1295	0.1 ^c	1.3			-106.9756	<0.1 ^c	-107.2496	0.1 ^c	-107.2576	0.1 ^c	
			0.4 ^f			0.6 ^f				-106.9685 ^a	0.3 ^f	-107.1934 ^a	0.5 ^f	-107.1986 ^a	0.6 ^f	
BN	$^1\Sigma^+$	-78.8826	0.1 ^h	2.4	-79.1896	0.6 ^h	nc ^f	-79.1403	0.2 ⁱ	-78.9036	0.1 ⁱ	-79.2407	0.7 ⁱ	-79.2814	0.7 ⁱ	-79.0884
			0.1 ⁱ			<0.1 ⁱ				-78.8992 ^a	0.3 ^h	-79.2039 ^a	0.5 ^h	-79.2445 ^a	0.4 ^h	
LiH	$^1\Sigma^+$	-7.9813	0.2	1.8	-8.0022	0.2	1.9			-7.9860	0.1	-8.0132	0.1	-8.0209	0.1	

^aEnergies obtained using the 6-311G(d,p) basis set. ^bIn HeBeO. ^cIn HeLiF. ^dIn NeBeO. ^eIn ArBeO. ^fIn ArLiF. ^gIn HeLiH. ^hIn ArBN. ⁱIn HeBN. ^jFor HeBN, ArBN, and BN MP3/6-31G(d,p) optimized geometries are used. ^kNot completely optimized; see text. ^lNot converged.

Table II. Theoretically Predicted and Experimentally Obtained Equilibrium Distances r_e (in Å) for NGAB and AB Molecules

NGAB, AB	r_e	calculated				expt ^a
		HF/ 6-31G(d,p)	MP2/ 6-31G(d,p)	MP3/ 6-31G(d,p)	CAS/ 6-31G(d,p)	
HeBeO	He-Be	1.571	1.538		1.557	
	Be-O	1.296	1.347		1.332	
NeBeO	Ne-Be	1.779	1.758			
	Be-O	1.297	1.347			
ArBeO	Ar-Be	2.105	2.036			
	Be-O	1.298	1.347			
BeO	Be-O	1.295	1.356		1.336	1.330
HeLiF	He-Li	2.169	2.110			
	Li-F	1.555	1.567			
ArLiF	Ar-Li	2.684	2.467			
	Li-F	1.556	1.567			
LiF	Li-F	1.555	1.567			1.563
HeBN	He-B	1.267	3.509	1.279	3.050 ^b	
	B-N	1.219	1.326	1.250	1.292 ^b	
ArBN	Ar-B	1.858	1.900	1.847		
	B-N	1.222	1.291	1.250		
BN	B-N	1.239	1.325	1.276	1.291	1.283
HeLiH	He-Li	2.289	2.208			
	Li-H	1.629	1.622			
LiH	Li-H	1.630	1.623			1.596

^aReference 37. ^bNot completely optimized (see text).

Table III. Calculated Dissociation Energies D_0 Corrected by BSSE (in kcal/mol)

	6-31G(d,p)			6-311G((2df,2pd) ^a			CAS/ 6-31G(d,p)
	HF/	MP2/	MP3/	HF/	MP2/	MP4/	
HeBeO → He + BeO	2.8	2.3		3.7	3.3	2.6(3.1) ^d	3.5 ^b
NeBeO → Ne + BeO	6.9	4.6		3.5	3.2	2.2	
ArBeO → Ar + BeO	7.9	7.8		7.6	7.8	7.0	
HeLiF → He + LiF	0.1	<0.1		<-0.1	<-0.1	0.1	
ArLiF → Ar + LiF	0.7	0.3		-0.2	0.1	<0.1	
HeBN → He + BN	6.1	<0.1 ^b	-1.2 ^c	8.5 ^e	-14.4 ^e	-25.4 ^e	<0.1 ^b
ArBN → Ar + BN	14.2	-7.7 ^b	8.9 ^c	15.5 ^e	-5.1 ^e	-17.2 ^e	
HeLiH → He + LiH	-0.1	-0.2		-0.2	-0.1	-0.1	

^a At MP2/6-31G(d,p) optimized geometries. ^b D_0 value (without ZPE correction). ^c Using HF/6-31G(d,p) frequencies. ^d Using ZPE and geometry optimized at MP4(SDQ)/6-311G(2d,2p) as shown in Table IV. ^e Using HF/6-31G(d,p) frequencies and MP3/6-31G(d,p) optimized geometries.

Table IV. Optimized Equilibrium Distances (in Å) for HeBeO (1) and BeO at Various Levels of Theory Using Analytical Gradients

	E_{tot}	r_{BeO}	r_{HeBe}
(a) HeBeO (1)			
HF/6-31G(d,p)	-92.2710	1.296	1.571
MP2/6-31G(d,p)	-92.5428	1.347	1.538
MP3/6-31G(d,p)	-92.5318	1.314	1.536
MP4(SDQ)/6-31G(d,p)	-92.5488	1.344	1.541
CASSCF/6-31G(d,p)	-92.4252	1.332	1.577
MP4(SDQ)/6-311G(2d,2p)	-92.6525	1.333	1.519
(b) BeO			
HF/6-31G(d,p)	-89.4091	1.295	
MP2/6-31G(d,p)	-89.6547	1.356	
MP3/6-31G(d,p)			
MP4(SDQ)/6-31G(d,p)	-89.6546	1.358	
CASSCF/6-31G(d,p)	-89.5644	1.336	
MP4(SDQ)/6-311G(2d,2p)	-89.7483	1.341	
exptl ^a		1.331	

^a Reference 37.

Be-O distance is predicted to be shorter in **1** than in BeO. As for the He-Be distance in **1**, CAS/6-31G(d,p) and MP4(SDQ)/6-311G(2d,2p) differ considerably. The former method predicts a distance of 1.577 Å, while the latter methods predicts a distance of 1.519 Å (Table IV). Since MP4 accounts for a considerable part of correlation corrections and since the larger basis set was used at this level of theory, we consider the MP4(SDQ)/6-311G(2d,2p) result to be more reliable. When this geometry is used for the calculation of the dissociation energy at MP4(SDQ)/6-311G(2df,2pd) and corrected for BSSE and ZPE effects, a value of 3.1 kcal/mol is obtained.

In order to further characterize and aid in the identification of HeBeO, we calculated the infrared spectra of **1** and BeO. Unscaled (harmonic) vibrational frequencies and IR intensities are shown in Table V. The identification of **1** with the aid of infrared spectroscopy may be achieved by considering (i) that there are two additional frequencies in **1** and (ii) that the Be-O stretching mode in **1** is shifted relative to that of BeO. The theoretically predicted IR spectra for BeO and HeBeO illustrate this (Figure 1). At the MP4(SDQ)/6-311G(2d,2p) level, the frequency of the Be-O stretching mode in isolated BeO is calculated to be 1410 cm⁻¹, 54 cm⁻¹ lower than the experimental value³⁷ of 1464 cm⁻¹. The MP2/6-31G(d,p) value is 1400 cm⁻¹. At both levels of theory listed in Table V, the frequency of the Be-O stretching mode is predicted to shift to higher values by more than 100 cm⁻¹, i.e., 114 cm⁻¹ at MP2/6-31G(d,p) and 124 cm⁻¹ at MP4(SDQ)/6-311G(2d,2p). With the experimental value for BeO³⁷ being 1464 cm⁻¹, the Be-O stretching frequency in **1** should be close to 1585 cm⁻¹. Its intensity should be one-third of that for BeO (Table V and Figure 1). The lower-lying vibrational frequencies of HeBeO, ν_2 and ν_3 , are calculated to be 505 and 212 cm⁻¹ at MP4(SDQ)/6-311G(2d,2p) (Table V, Figure 1). The corresponding values at MP2/6-31G(d,p) differ by ca. 20 cm⁻¹ (Table V). The calculated intensities for the vibrational modes of **1** reveal that the π -symmetric mode ν_3 has the highest infrared intensity and that the low-lying σ -symmetric mode ν_2 is hardly visible in the IR spectrum.

Table V. Theoretically Predicted Vibrational Frequencies ν (in cm⁻¹) and Infrared Intensities I (in km/mol) for HeBeO, NeBeO, ArBeO, and BeO

	ν_1	ν_2	ν_3	I_1	I_2	I_3
(a) HeBeO (1)						
MP2/6-31G(d,p)	1514(σ)	484(σ)	234(π)	3.6	1.4	39.3
MP4(SDQ)/6-311G- (2d,2p)	1534(σ)	505(σ)	212(π)	6.9	0.4	66.3
(b) NeBeO (2)						
MP2/6-31G(d,p)	1521(σ)	314(σ)	185(π)	9.7	2.4	89.7
(c) ArBeO (3)						
MP2/6-31G(d,p)	1534(σ)	296(σ)	190(π)	35.9	4.9	73.7
(d) BeO						
MP2/6-31G(d,p)	1400(σ)			22.8		
MP4(SDQ)/6-311G- (2d,2p)	1410(σ)			23.5		
exptl ^a	1464(σ)					

^a Reference 37.

Table VI. Results of the Electron Density Analysis Calculated at MP2/6-31G(d,p)^a

	r_e	ρ_b	$\nabla^2\rho_b$	H_b
(a) HeBeO (1)				
HeBe	1.538	0.171	6.67	+0.100
BeO	1.347	1.145	41.62	-0.165
(b) NeBeO (2)				
NeBe	1.758	0.175	6.84	+0.075
BeO	1.347	1.144	41.46	-0.168
(c) ArBeO (3)				
ArBe	2.036	0.237	5.61	+0.020
BeO	1.347	1.150	41.04	-0.173
(d) BeO				
BeO	1.356	1.105	40.60	-0.136
(e) HeBe ²⁺				
HeBe	1.453	0.284	9.06	+0.120
(f) NeBe ²⁺				
NeBe	1.619	0.333	11.56	+0.102
(g) ArBe ⁺				
ArBe	2.045	0.270	4.88	-0.005
(h) ArBe ²⁺				
ArBe	1.857	0.504	9.09	-0.082

^a Interatomic distances r_e (in Å), electron density ρ_b (in e/Å³), Laplacian $\nabla^2\rho_b$ (in e/Å⁵), and energy density H_b (in hartrees/Å³) at the critical point r_b .

We investigated the electronic structure of **1** in comparison with that of BeO by analyzing the electron density distribution $\rho(\mathbf{r})$ and its associated Laplace distribution $\nabla^2\rho(\mathbf{r})$ of both compounds at their MP2/6-31G(d,p) geometries. Table VI summarizes the results of the one-electron density analysis. Figure 2 depicts contour line diagrams of the Laplace distribution of **1** and BeO. They suggest a strong charge transfer from Be to O both in **1** and BeO. The Laplace distribution is no longer spheric but indicates

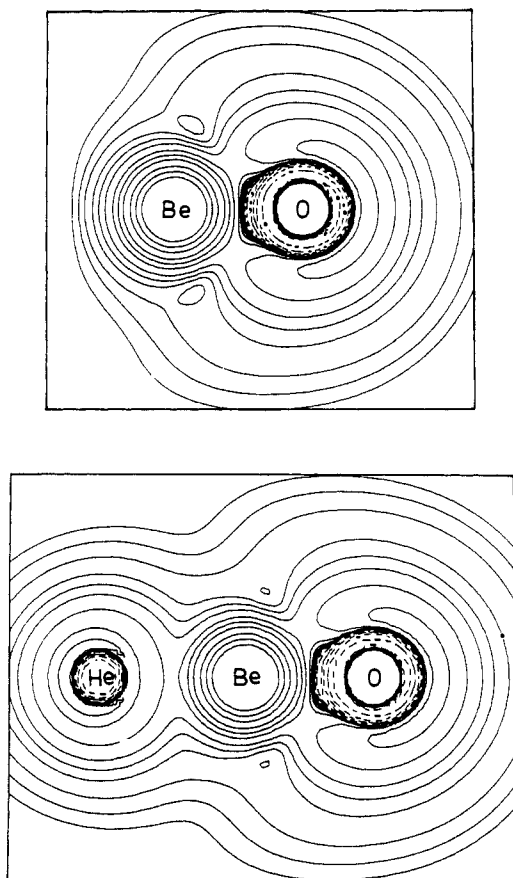


Figure 2. Contour line diagrams of the Laplace concentration $-\nabla^2\rho(r)$ of (a) BeO and (b) HeBeO (1) at MP2/6-31G(d,p). Dashed contour lines are in regions of charge concentration and solid lines in regions of charge depletion. Inner-shell concentrations are not shown.

a large buildup of negative charge in front of the O atom. The computed H_b values are <0 but rather small, similar to the values found for Be–C bonds in C_2Be , C_2Be_2 , and related compounds.³⁴ We conclude that the BeO bond in **1** and BeO, although covalent, possesses partial ionic character.

The Laplace field of He in **1** is almost identical with that of isolated He (Figure 2). Inspection of the (solid) contour lines in Figure 2, however, suggests that the electron density of He is polarized toward BeO, indicative of dipole-induced dipole interactions. This is confirmed by the value of $H_b(\text{HeBe}) > 0$, which is typical of electrostatic interactions (Table VI). The analysis of the electron density distribution of HeBeO suggests that *there is no covalent bond between He and Be*.

NeBeO (2) and ArBeO (3). What changes can be expected when He in **1** is replaced by the heavier noble-gas elements neon or argon, i.e., when NeBeO (2) and ArBeO (3) are formed? Since the polarizabilities increase³⁹ in the order $\text{He} < \text{Ne} < \text{Ar}$, the stabilities of the respective NGBEO structures toward dissociation may be expected to follow the same trend, i.e., $1 < 2 < 3$. As for donor–acceptor interactions¹⁶ between NG and BeO, one has to consider that the energy of the highest occupied orbital (HOMO) rises from He to Ne and Ar, thus inducing larger stabilizing HOMO–LUMO interactions with the acceptor BeO. However, Ne and Ar possess (filled) p orbitals in their valence shells which are absent for He. Therefore, repulsive $p-\pi$ interactions involving the occupied 1π MOs of BeO are possible in **2** and **3**, but not in **1**.

The calculated dissociation energies D_0 shown in Table II indicate that both **2** and **3** are stable toward dissociation just like **1**. At the highest level of theory listed in Table II, **2** is stable by

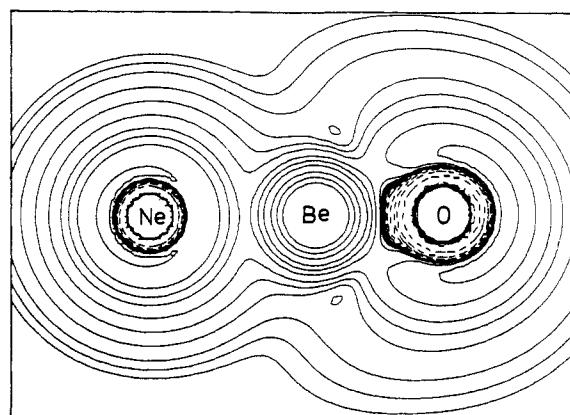


Figure 3. Contour line diagrams of the Laplace concentration $-\nabla^2\rho(r)$ of NeBeO (2) at MP2/6-31G(d,p). See also caption to Figure 2.

2.2 kcal/mol and **3** by 7.0 kcal/mol. The D_0 value for **2** is slightly smaller than that for **1**. However, BSSE corrections for **2** and **3** are much higher than for **1** (Table I). In case of **2**, the dissociation energy of 2.2 kcal/mol results from a BSSE correction of 5.8 kcal/mol. While the use of the full counterpoise method to correct for the BSSE has been justified,^{26b,c} there are arguments which suggest that the BSSE might be overestimated by this procedure.⁴⁰ This is because the counterpoise method uses the *full* basis set of the complete molecule XY rather than just the basis set of X augmented by the virtual orbitals of Y^{26,40} to calculate the energy of the respective fragment X. In the particular case considered here, the outer basis functions of Y, i.e., those of Be and O, are of the right size to describe the valence region of Ne but not that of He or Ar. As a consequence, the counterpoise method leads to a larger BSSE correction for Ne than for He and Ar.

The dissociation energies D_0 calculated here should therefore be considered as lower bounds to the true D_0 values. The difference in the calculated stabilities for **1** and **2** is not sufficient to safely conclude which of the two compounds is more stable. But considering calculated BSSE values we believe that NeBeO is more stable than HeBeO. However, the much larger value predicted for **3** ($D_0 = 7.0$ kcal/mol) establishes that ArBeO is more stable than both HeBeO and NeBeO. It is gratifying that the calculated stability of **3** changes very little at all levels of theory shown in Table III.

Except for the NG–Be distance, the calculated properties for **2** and **3** are similar to **1**. The Be–O distance is predicted to be the same for the three compounds, i.e., 1.347 Å (Table II). The BeO stretching frequency ν_1 is calculated to be (unscaled) 1521 cm^{-1} for **2** and 1534 cm^{-1} for **3** (Table V), in line with an upfield shift of ca. 120 cm^{-1} relative to BeO. Interestingly, the infrared intensity of this mode I_1 is calculated to be lower for **1** and **2**, but higher for **3** compared with isolated BeO (Table V). The sequence $I_1 < I_2 < I_3$ corresponds to an increase in the dipole moments μ ($\mu(1) = 5.40$; $\mu(2) = 6.49$; $\mu(3) = 7.43$ D at MP2/6-31G(d,p)) which indicates an increase in charge transfer $\text{NG} \rightarrow \text{Be} \rightarrow \text{O}$ in NGBEO. The frequencies of ν_2 and ν_3 are lower for **2** and **3** than for **1**. For all three compounds the computed IR intensity of ν_2 is very small, but rather large for ν_3 .

The analysis of the one-electron density distribution reveals that the electronic structures of **1**, **2**, and **3** are very similar. The calculated electron density ρ_b suggests an increase in NG–Be interactions in the order $1 < 2 < 3$ (Table VI), which is also reflected by the corresponding energy density H_b that approaches zero, indicating a change possibly toward beginning covalency. In agreement with these data, the contour levels of the Laplacian distribution for **2** and **3** reveal an increasing deformation of the valence sphere of the noble-gas atom toward BeO when going from **1** to **3** (Figure 2–4) typical of the onset of covalent bonding.

(39) Miller, T. M.; Bederson, B. *Advances in Atomic and Molecular Physics*; Bates, D. R., Bederson, B., Eds.; Academic Press: New York, 1977; Vol. 13, p 1f.

(40) (a) Johansson, A.; Kollman, P.; Rothenberg, S. *Theor. Chim. Acta* 1973, 29, 167. (b) Senff, U. E.; Burton, P. G. *J. Phys. Chem.* 1985, 89, 797. Further references are found in ref 26a.

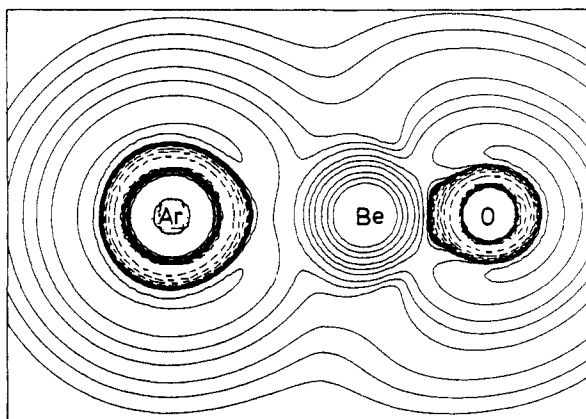


Figure 4. Contour line diagrams of the Laplace concentration $-\nabla^2\rho(r)$ of ArBeO (3) at MP2/6-31G(d,p). See also caption to Figure 2.

However, H_b is positive for both 1, 2, and 3 (Table VI), thus suggesting a predominance of electrostatic bonding forces even for the heavier NG atoms Ne and Ar.

HeLiF (4) and ArLiF (5). In search of molecules other than BeO possibly capable of binding the light noble-gas elements, we investigated the isoelectronic LiF in its $1\Sigma^+$ ground state.³⁷ We optimized HeLiF (4) and ArLiF (5) at HF/6-31G(d,p) and MP2/6-31G(d,p). The results shown in Table II reveal that both levels of theory predict significantly longer distances NG-Li in 4 and 5 compared to NG-Be distances in 1 and 3. At MP2/6-31G(d,p), the He-Li distance is calculated as 2.110 Å, and the Ar-Li distance as 2.467 Å (Table II), ca. 0.5 Å longer than the corresponding He-Be and Ar-Be distances in 1 (1.538 Å) and 3 (2.036 Å). As a consequence, the calculated dissociation energies for 4 and 5 are vanishingly small (0.1 and <0.1 kcal/mol, Table III). The LiF bond length is calculated the same in 4 and 5, and in isolated LiF. It is obvious that LiF does not interact with He and Ar as strongly as BeO does, and the same can be expected for NeLiF. Possible reasons for the differences in the interactions of BeO and LiF with the noble-gas atoms are discussed below.

HeBN (6) and ArBN (7). Another potential binding partner for the light noble-gas elements which is isoelectronic to BeO and LiF is boron nitride, BN. Therefore, we have investigated the interactions between He and Ar and the $1\Sigma^+$ state⁴¹ of BN in the adducts HeBN (6) and ArBN (7).

The investigation of 6 and 7 exhibited some computational problems which did not allow a straightforward theoretical treatment analogous to 1-5. The data in Tables II and III show that HF/6-31G(d,p) predicts a rather short (1.267 Å) He-B distance for 6 with a D_0 value of 6.1 kcal/mol, while MP2/6-31G(d,p) suggests a much larger (3.509 Å) He-B distance and $D_0 < 0.1$ kcal/mol.⁴² Qualitatively different results are predicted for the stability and geometry of HeBN at these two levels of sophistication. However, both methods describe the bond length of isolated BN poorly. While the experimental value³⁷ is 1.283 Å, the B-N distance is calculated significantly too short (1.239 Å) at HF/6-31G(d,p) and too long (1.325 Å) at MP2/6-31G(d,p).

Better agreement with experiment is obtained at MP3/6-31G(d,p), which leads to a B-N distance of 1.276 Å (Table II) close to the experimental value of 1.283 Å. Optimization of 6 at MP3/6-31G(d,p) yielded a structure with a very short He-B distance (1.279 Å) similar to the value found at HF/6-31G(d,p). However, the calculated dissociation energy D_0 for 6 at MP3/6-31G(d,p) indicates that HeBN is not a stable molecule. While

the D_e value is still positive, D_0 is -1.2 kcal/mol (Table III). Single-point calculations at MP4(SDTQ)/6-311G(2df,2pd) even predict dissociation of 6 into He and BN to be exothermic by 25.4 kcal/mol. Thus, 6 is not a stable species.

In order to verify this result, we performed full-valence CASSCF calculations using the 6-31G(d,p) basis set. At this level of theory, the He-B distance is >3.05 Å (not fully optimized) and the corresponding dissociation energy only 0.1 kcal/mol. Inspection of the coefficients for the dominant configurations of the MCSCF wave function for BN ($1\Sigma^+$) showed that besides the leading configuration ($c = 0.901$) there are four other terms with coefficients >0.10. The insufficient description of the $1\Sigma^+$ state of BN by a single-determinant approach is probably the reason why the perturbational treatment of BN and NGBN structures leads to conflicting results. In a recent CI study by Karna and Grein^{43a} of the low-lying states of BN, it has been noted that the CI wave function of ($1\Sigma^+$) BN consists only of 71% of the Hartree-Fock configuration.

The calculation of ArBN (7) posed similar problems. Geometry optimizations at HF/6-31G(d,p) and MP2/6-31G(d,p) predict rather short Ar-B distances of 1.858 and 1.900 Å, respectively (Table II). Both values are smaller than the Ar-Be distance in 3 (Table II). At the MP2/6-31G(d,p) level, dissociation of 7 is calculated to be exothermic by 7.7 kcal/mol (Table III). A very small barrier (<1 kcal/mol) was calculated at MP2/6-31G(d,p), which is probably a computational artifact without physical meaning.

The geometry optimization of 7 at the MP3/6-31G(d,p) level also yields a geometry with a rather short (1.847 Å) Ar-B distance. At the same level, 7 is predicted to be stable toward dissociation by 8.9 kcal/mol (Table III). Single-point energy calculations at MP4(SDTQ)/6-311G(d,p) using the MP3/6-31G(d,p) optimized structure predict that 7 is by 17.2 kcal/mol unstable. Unlike 6, which is calculated as unstable at all correlated levels, no definite conclusion concerning the stability of 7 can be drawn from our calculations. However, the comparison of HeBeO (1) and HeBN (6) at the CASSCF level indicates that BN ($1\Sigma^+$) is not as strong a Lewis acid as BeO ($1\Sigma^+$).

HeLiH (8). We also included 8 in our study of neutral systems containing a light noble-gas atom because 8 had previously^{10a} been predicted to be a stable structure with a He-Li equilibrium distance of 1.60 Å and a stabilization energy of 1.6 kcal/mol. However, the corresponding calculations^{10a} had been performed at the HF level without corrections for BSSE and ZPE. The calculated data shown in Tables I-III indicate that 8 possesses a long He-Li equilibrium distance (2.208 Å at MP2/6-31G(d,p)) and a stabilization energy which, after correction for BSSE and ZPE, becomes even slightly negative (Table III). LiH interacts with He much less than BeO and is comparable in strength with those in HeLiF and HeBN.

4. Nature of Atom-Atom Interactions in Noble-Gas Structures 1-8

After presenting our results for structures 1-8, the remaining question to be answered concerns the type of interaction which prevails in these systems. Is the stability of 1-8 *solely* caused by dipole-induced dipole interactions^{26b,c} which classifies these structures as van der Waals (vdW) complexes, or is there a need to invoke orbital effects indicating truly chemical bonding? We will discuss this question in some detail because the answer to it provides important information as to whether there are neutral, *chemically bound* compounds of the light noble-gas elements which are stable in their ground state. However, it should be pointed out that such a discussion concerns chemical models rather than physical realities. Covalency is not an observable quantity, and while the underlying physical laws of chemical bonding are known from molecular quantum mechanics, there is no clear definition which allows one to distinguish uniquely between a weakly bound (chemical) molecule and a vdW complex.

(41) Unlike isoelectronic BeO and LiF, BN has a 3Π ground state.^{37,43} Because we are concerned with the interactions of the light noble-gas atoms (NG) with diatomics AB in their $1\Sigma^+$ state, it is irrelevant for our theoretical study if the $1\Sigma^+$ state is the ground or excited state. The 3Π state is a weaker Lewis acid than the $1\Sigma^+$ state, because the former has one more electron in a σ orbital.

(42) Because of convergence failure, the vibrational frequencies and, consequently, ZPE values for BN and HeBN at MP2/6-31G(d,p) could not be calculated.

(43) (a) Karna, S. P.; Grein, F. *Chem. Phys.* **1985**, *98*, 207. (b) Karna, S. P.; Grein, F. *Mol. Phys.* **1985**, *56*, 641.

Table VII. Calculated Total Energies E_{tot} (in hartrees), Electron Affinities EA (in eV), and Dipole Moments μ (in Debye) in Comparison with Other Experimental/Calculated Results

struct.	HF			MP2			MP3			exptl calcd	
	E_{tot}^a	EA ^a	μ^b	E_{tot}^a	EA ^a	μ^b	E_{tot}^a	EA ^a	μ^b	EA	μ
LiF	-106.9462	0.31	6.22	-107.1512	0.33	5.85				0.31 ^c	6.33 ^d
LiF ⁻	-106.9575			-107.1632							
BeO	-89.4160	2.01	6.78	-89.6648	1.98	5.40				2.15 ^e	7.1 ^e
BeO ⁻	-89.4898			-89.7376							
BN	-78.8875	4.33	4.39	-79.1957	1.85	1.34	-79.1458	3.33	2.81		2.03 ^f
BN ⁻	-79.0465			-79.2636			-79.2683				
LiH	-7.9815	0.21	5.95	-8.0018	0.23	5.79				0.3 ^g	5.88 ^h
LiH ⁻	-7.9893			-8.0101							

^a 6-31+G(d,p) basis set. ^b 6-31G(d,p) basis set. ^c Δ SCF value taken from ref 57. ^d Experimental value from ref 47. ^e Experimental value from ref 49. ^f Calculated (CI) value from ref 43a. ^g Calculated value from ref 46b. ^h Experimental value from ref 48.

Many examples of vdW complexes containing light noble-gas atoms are known,^{13,14} and the experimental information concerning their stabilities is similar to what is calculated here for structures 4–8. For example, the dissociation energy D_0 of ArNO in its $X^2\Pi$ ground state was experimentally determined as 87 cm⁻¹ (0.25 kcal/mol).^{13b} Based on this result and the atomic polarizabilities,³⁹ D_0 values for HeNO and NeNO have been estimated as 8.5 cm⁻¹ (0.02 kcal/mol) and 20 cm⁻¹ (0.06 kcal/mol).^{13b} For NeHCl and ArHCl, experimental results of 68 cm⁻¹ (0.19 kcal/mol) and 180 cm⁻¹ (0.51 kcal/mol), respectively, have been reported.¹⁴ A D_0 value of 214 cm⁻¹ (0.61 kcal/mol) has experimentally been obtained for ArHF.^{14d}

Also the interatomic distances found for many vdW complexes are comparable to those calculated for 4–8. ArNO has a “T”-shaped geometry with an intranuclear distance of 3.65 Å and an angle of 95° to the NO axis.^{13a} NeHCl and ArHCl possess both a linear geometry with experimentally determined distances between the noble-gas atom and the center of mass of HCl of 3.764 Å for NeHCl and 4.009 Å for ArHCl.^{14f} This corresponds to interatomic distances of ~2.55 Å (NeH) and ~2.80 Å (ArH). An extensive theoretical treatment of NeHF predicts also a linear geometry with a Ne–H distance of ~2.92 Å and a well depth of ~11.4 cm⁻¹ (0.03 kcal/mol).⁴⁴ Our calculated results for structures 4–8 point to a similar range of stabilities and interatomic distances. The stabilization energies calculated for 4–8 can be explained in terms of long-range interactions which classify them as vdW complexes.

But what about the NGBeO systems 1, 2, and 3? The theoretical results presented here indicate substantially shorter noble-gas distances and higher dissociation energies for 1–3 than for 4–8. The D_0 value of 7.0 kcal/mol predicted for ArBeO is much higher than what is found for any Ar-containing vdW complex.

Chemical bonds with dissociation energies of less than 10 kcal/mol are discussed in the literature. For example, the NO–NO₂ dissociation energy D_0 is only 9.5 kcal/mol.^{45a} The diatomic molecules XeO, XeN, and XeF are considered as chemical compounds although their D_0 values are only 8.7, 5.5, and 4.0 kcal/mol.⁴⁵ A thorough discussion of bonding features in these compounds is missing up to date and, therefore, their classification is somewhat arbitrary. On the other hand, one cannot exclude that the classification is correct, which means that the designation of weak interactions (<10 kcal/mol) if they are chemical, i.e., covalent, or not, cannot be based on dissociation energies alone.

Chemical interactions in helium compounds have successfully been rationalized using the model of donor–acceptor interactions,^{16–18} and it also seems to be a valuable model for the chemistry of neon and argon.^{8b} If applied here, the acceptor ability of BeO toward He, Ne, and Ar should be stronger than the acceptor ability of LiF, BN, and LiH. The relative electron affinities (EA) of the four diatomics might be used as a measure

for their different affinities toward a Lewis base. Table VII shows the calculated vertical EA values at the same level of theory used for the geometry optimizations but with inclusion of diffuse orbitals, which is necessary for an adequate theoretical treatment of anions.⁴⁶ If long-range forces are dominant in structures 1–8, the dipole moments of BeO, LiF, BN, and LiH should account for the calculated differences. Table VII shows our theoretically predicted dipole moments of the diatomic molecules together with the results of earlier calculations and experimentally observed data as far as available.

At MP2/6-31G(d,p), LiF (5.85 D) and LiH (5.79 D) have larger dipole moments than BeO (5.40 D) and especially BN (1.34 D). Experimental values for LiF (6.33 D)⁴⁷ and LiH (5.88 D)⁴⁸ are in satisfactory agreement with our calculated results. For BeO, the theoretically predicted dipole moment at MP2/6-31G(d,p) is lower than the experimentally obtained⁴⁹ value of 7.1 ± 0.3 D. There is no experimental value available for the dipole moment of BN ($^1\Sigma^+$). Our calculated dipole moment for BN is smaller than the previously reported^{43a} value of 2.03 D estimated at SCF + CI. The theoretically predicted electron affinities at MP2/6-31+G(d,p) are in case of LiF (0.33 eV), BeO (1.98 eV), and LiH (0.23 eV) in very good agreement with previous theoretical treatments (Table VII). Concerning the electron affinity of BN ($^1\Sigma^+$), no value was found in the literature.⁵⁰

It was pointed out by one referee that the calculated dipole moment and electron affinity obtained for BN at the MP2 level are not reliable because a one-determinant description of BN is not appropriate. We agree with this, but our theoretical prediction that BN has a much smaller dipole moment than BeO, LiF, and LiH is supported by the experimental results (Table VII). The reason that we present the calculated dipole moments and electron affinities using one-determinant methods also for BN is to show the correlation between calculated electron affinity and dipole moments and the predicted geometries for NGBN at the same level of theory. This is discussed in detail below.

If only dipole-induced dipole forces are considered to be responsible for the attractive NG–AB interactions in 1–8, NGLiF and NGLiH should exhibit the largest dissociation energies in contradiction to the calculated results shown in Table III. However, as discussed below when applying formula 1 for the calculation of the interaction energies, this is only valid for ideal dipoles. An incoming NG atom “sees” not only the dipole moment of AB but also the positive charge at atom A. The larger the charge at these atoms is, the larger are interactions between NG and A. For Li, the maximal charge in LiF and LiH is +1. For Be, however, the positive charge in BeO may be larger than +1. The discussion above suggests⁵¹ that it is larger than in NGBe⁺

(46) (a) Clark, T.; Chandrasekhar, J.; Spitznagel, G. W.; Schleyer, P. v. R. *J. Comput. Chem.* **1983**, *4*, 294. (b) Frenking, G.; Koch, W. *J. Chem. Phys.* **1986**, *84*, 3224.

(47) Stogryn, D. E.; Stogryn, A. P. *Mol. Phys.* **1966**, *11*, 371.

(48) Wharton, A.; Gold, L. P.; Klemperer, W. *J. Chem. Phys.* **1960**, *33*, 1255.

(49) Yoshimine, M. *J. Phys. Soc. Jpn.* **1968**, *25*, 1100.

(50) For the $X^3\Pi$ state of BN the calculated electron affinity has been reported.^{43a}

(44) Fowler, P. W.; Buckingham, A. D. *Mol. Phys.* **1983**, *50*, 1349.

(45) (a) Kerr, J. A. *Chem. Rev.* **1966**, *66*, 465. (b) Herman, R.; Herman, L. *J. Phys. Radium* **1963**, *24*, 73. (c) Kondratiev, V. N. *Bond Dissociation Energies, Ionization Potentials and Electron Affinities*; Mauka Publishing House: Moscow, 1974. (d) Aquilanti, V.; Luzzatti, E.; Pirani, F.; Volpi, G. *G. Chem. Phys. Lett.* **1982**, *90*, 382.

Table VIII. Calculated Interatomic Distances r_e (in Å), Total Energies E_{tot} (in hartrees), ZPE and BSSE Corrections and Dissociation Energies D_0 (in kcal/mol) for Diatomic Cations $X\text{Be}^{n+}$ ($X = \text{He, Ne, Ar; } n = 1, 2$) in Their Electronic Ground States. Inductive Interaction E_{ind} Calculated via eq 2 (in kcal/mol)

struct	symm	MP2/6-31G(d,p)			MP4/6-311G(2df,2pd) ^a				
		r_e	E_{tot}	ZPE	E_{tot}	BSSE	D_e^b	D_0^b	E_{ind}
HeBe ⁺	X ² Σ ⁺	3.132	-17.1597	0.1	-17.1740	0.1	0.3	0.2	0.4
HeBe ²⁺	X ¹ Σ ⁺	1.453	-16.5241	1.2	-16.5400	0.2	20.1	18.9	30.5
NeBe ⁺	X ² Σ ⁺	1.856	-142.9140	0.4	-143.0694	4.2	-0.1	-0.5	5.5
NeBe ²⁺	X ¹ Σ ⁺	1.619	-142.2977	1.0	-152.2401	5.1	28.7	27.7	38.2
ArBe ⁺	X ² Σ ⁺	2.045	-541.2154	0.5	-541.3271	1.6	10.7	10.2	15.6
ArBe ²⁺	X ¹ Σ ⁺	1.857	-540.6426	1.0	-540.7525	1.9	67.6	66.6	91.5
Be ⁺	² S		-14.2786		-14.2762				
Be ²⁺	¹ S		-13.6127		-13.6104				
He	¹ S		-2.8806		-2.8972				
Ne	¹ S		-128.6262		-128.7867				
Ar	¹ S		-526.9200		-527.0313				

^a Full fourth-order (SDTQ) at MP2/6-31G(d,p) optimized geometries. ^b Calculated for the dissociation reactions $\text{NGBe}^{n+} \rightarrow \text{NG} + \text{Be}^{n+}$.

and lower than in NGBe^{2+} . Accordingly, electrostatic interactions should be much stronger in the case of BeO than for either LiF or LiH .⁵²

However, we cannot exclude that donor-acceptor interactions enhance the stability of some of these structures. BeO differs from LiF and LiH not only by a higher positive charge at Be than at Li , but it also has a significantly higher electron affinity (Table VII). This is due to the LUMO of BeO , the low-lying 5σ MO in the $^1\Sigma^+$ state which possesses distinct Be-O bonding character. Any HOMO-LUMO interactions involving the occupied $p(\sigma)$ orbitals of NG ($1s$ AO for He) would lead to a charge transfer from NG to $\sigma(\text{BeO})$ which should result in a shortening of the Be-O distance in 1-3 relative to isolated BeO . This is, indeed, found for 1-3 at the correlated levels of theory (Tables II and IV). The calculated electron affinities for BN may also explain the dramatic differences found for HeBN at $\text{HF}/6-31\text{G}(\text{d,p})$ and $\text{MP2}/6-31\text{G}(\text{d,p})$. Both methods predict the lowest dipole moment for BN of the four diatomics AB (Table VII). The calculated electron affinity, however, is much higher at $\text{HF}/6-31\text{G}(\text{d,p})$ (3.71 eV) than for BeO (1.51 eV) while at $\text{MP2}/6-31\text{G}(\text{d,p})$ it is lower (1.85 eV) than for BeO (1.98 eV). At the $\text{MP3}/6-31\text{G}(\text{d,p})$ level, the electron affinity of BN is significantly higher (3.33 eV) than at $\text{MP2}/6-31\text{G}(\text{d,p})$. The oscillating EA values for BN run parallel to the calculated He-B distances (Table II).

There are some characteristics of long-range (vdW) forces which help to analyze weakly interacting systems. Long-range interactions between neutral or charged atoms or molecules are caused by permanent or induced electric dipole moments and may be described by the equations of classical electrostatics.⁵² The interaction energy E_{ind} between a neutral atom X and a molecule AB which has a permanent dipole moment μ_{AB} is given by:⁵³

$$E_{\text{ind}} = -0.5\alpha_X\mu_{\text{AB}}^2(1 + 3\cos^2\theta)/\pi\epsilon_0r_{\text{X,AB}}^6 \quad (1)$$

Here, α_X is the electric dipole polarizability of atom X , ϵ_0 is the dielectric constant, $r_{\text{X,AB}}$ is the distance between X and AB , and θ is the angle between the direction of the dipole moment μ and the axis $X-\text{AB}$. In case of the linear NGBeO species, θ is 0. Thus, the interaction between X and AB is proportional to $r_{\text{X,AB}}^{-6}$. The recommended values³⁹ for the atomic polarizabilities of the noble-gas atoms are $\alpha(\text{He}) = 0.205 \text{ \AA}^3$, $\alpha(\text{Ne}) = 0.395 \text{ \AA}^3$, and $\alpha(\text{Ar}) = 1.64 \text{ \AA}^3$. The calculated dipole moment of BeO at $\text{MP2}/6-31\text{G}(\text{d,p})$ is 5.40 D (Table VII). Using the $\text{MP2}/6-31\text{G}(\text{d,p})$ optimized distances $r_{\text{X,AB}}$ between the noble-gas atoms and the midpoint of the BeO bond in structures 1-3, the theoretically predicted interaction energies E_{ind} via eq 1 are 1.5

kcal/mol for 1, 1.6 kcal/mol for 2, and 3.5 kcal/mol for 3. The E_{ind} values are lower than the calculated dissociation energies.

However, objections can be raised against using (1) for structures 1-3 because formula 1 is only valid for ideal dipoles and $r_{\text{X,AB}}$ being larger than $r_{\text{NG,BeO}}$ in 1-3. Therefore, the result $E_{\text{ind}} < D_e$ does not necessarily indicate covalent character for the NG-Be interactions. Nevertheless, it is interesting that E_{ind} deviates from D_e by more than 3 kcal/mol for 3 but just 1 kcal/mol for 1 and 2.

A common feature of long-range interactions is that they are rather isotropic. Therefore, vdW complexes are usually very flexible structures, triatomic species often have T-shaped structures, and the potential around the minimum is rather flat.^{13,14} This is in contrast to chemical compounds which are most often rather rigid because of an anisotropic distribution of the electron density of molecules. We calculated the structure and energy of 1 as a function of the bending angle τ . With $\tau = 120^\circ$, the He-Be equilibrium distance becomes very long (3.519 Å) with an interaction energy D_e of <0.1 kcal/mol ($\text{MP2}/6-31\text{G}(\text{d,p})$), which is similar to what is calculated for HeLiF and HeBN in their equilibrium geometry. This might point to a qualitatively different interaction in linear and bent HeBeO . However, when using formula 1, which is appropriate for longer He-Be distances, the interaction energy E_{ind} for the $\text{MP2}/6-31\text{G}(\text{d,p})$ optimized geometry at $\tau = 120^\circ$ is calculated to be 0.02 kcal/mol which agrees with the predicted D_e result.

It may be argued that because of the rather short NG-Be distance in 1-3, a more appropriate treatment would be to consider the interaction between the positively charged Be atom and the induced dipole moment in NG . In this context, it is illuminating to compare the dissociation energies calculated for 1-3 with the D_e values predicted for singly and doubly charged HeBe^{n+} , NeBe^{n+} , and ArBe^{n+} ($n = 1, 2$) for the dissociation⁵⁴ into $\text{NG} + \text{Be}^{n+}$ at the same level of sophistication. The calculated dissociation energies for the six diatomic cations^{5b,17} are shown in Table VIII.

The very low D_e value for ($X^2\Sigma^+$) HeBe^+ (0.3 kcal/mol) indicates that HeBe^+ is a vdW complex. In contrast, HeBe^{2+} is much stronger bound ($D_e = 20.1$ kcal/mol). Obviously, He-Be interactions in 1 are significantly stronger than in HeBe^+ but much weaker than in HeBe^{2+} . The same holds for 2 when compared with the respective diatomic cations NeBe^{n+} .⁵⁵ However, ArBe^+ has a calculated dissociation energy D_e of 10.7 kcal/mol, which is larger than D_e (3). For ArBe^{2+} , D_e is even 68 kcal/mol (Table VIII), but the magnitude of D_e does not necessarily imply that interactions between NG and Be are covalent. If one estimates the electrostatic attraction due to charge-induced dipole interactions between an atom X and an ion A which possesses the

(51) We do not use partial charges calculated by the Mulliken partitioning scheme because of the well-known deficiency especially for electronegative elements: Bachrach, S. M.; Streitwieser, A. *J. Am. Chem. Soc.* **1984**, *106*, 2283. For BeO , the partial atomic charge predicted by the Mulliken population analysis at $\text{MP2}/6-31\text{G}(\text{d,p})$ is only +0.47 for Be .

(52) For a more quantitative description of the electrostatic interactions, one has also to consider the atomic dipole and quadrupole moments.

(53) Hirschfelder, J. O.; Curtiss, C. F.; Bird, R. B. *Molecular Theory of Gases and Liquids*; Wiley: New York, 1964.

(54) In case of $\text{ArBe}^{2+}(X^1\Sigma^+)$, the lowest lying dissociation reaction yields $\text{Ar}^+(^2P) + \text{Be}^+(^2S)$.

(55) The negative dissociation energies calculated for NeBe^+ are caused by using different theoretical levels for the energy calculations ($\text{MP4}(\text{SDTQ})/6-311\text{G}(2\text{df},2\text{pd})$) than for the optimizations of the atomic distances ($\text{MP2}/6-31\text{G}(\text{d,p})$).^{5b}

charge q_A with the aid of the formula,⁵³

$$E_{\text{ind}} = -0.5\alpha_X q_A^2 / r_{XA}^4 \quad (2)$$

attraction energies 30–50% larger than calculated D_e values are found (Table VIII). This means that (i) the strength of the NG–Be interactions does not necessarily invoke other than electrostatic forces to explain the stability of NGBe^{n+} and (ii) for the calculated NG–Be distances of NGBe^{n+} , formula 2, which is only valid for point charges, provides no longer a quantitative description of interaction energies.

A necessary condition for the validity of the above discussion is that the atomic polarizabilities α of the noble gas atoms are calculated correctly at the theoretical level employed in the investigation. It has been found that at the MP4(SDTQ)6/311G-(2df,2pd) level the calculated α values for He, Ne, and Ar deviate less than 10% from experimental results if the complete basis set of the NGX^{n+} cation is employed.⁵⁶

The discussion of NG–BeO interactions using the experimental and theoretical results of the dipole moment and electron affinity of BeO points toward electrostatic interactions, although covalent contributions cannot completely be dismissed. Analysis of $\rho(r)$ and $\nabla^2\rho(r)$ for HeBe^{2+} , NeBe^{2+} , ArBe^+ , and ArBe^{2+} (Table VI) reveals that there is more density in the internuclear region than found for 1–3. Nevertheless, H_b values are either positive or close to zero (Table VI). When going from He to Ar, H_b becomes smaller (more negative), as has been found for 1–3. But even for ArBe^{2+} , the calculated H_b result is far from the typical value found for a covalent NG–X bond (e.g., -1.0 for some HeC bonds¹⁶). We conclude that despite the large D_e values (20–68 kcal/mol, Table VIII) all interactions in NGBe^{2+} are essentially electrostatic. *Since the partial charge of Be in NGBeO is definitely lower than*

2, it is reasonable to conclude that NG–Be interactions in 1–3 are also electrostatic.

5. Summary

Our theoretical results predict that HeBeO (1), NeBeO (2), and ArBeO (3) are stable toward dissociation of the noble-gas atom. The calculated dissociation energies D_0 at the highest level of theory used in our study and corrected by BSSE are 3.1 kcal/mol for 1, 2.2 kcal/mol for 2, and 7.0 kcal/mol for 3. These values are lower bounds to the correct D_0 values because the BSSE is probably overestimated by the counterpoise method. In contrast to the NGBeO structures 1–3, the NGLiF , NGBN , and HeLiH species 4–8 are calculated with much weaker NG–AB interactions, ≤ 0.1 kcal/mol.

The weakly interacting NG–AB systems 4–8 should be considered as van der Waals complexes which are bound by dipole-induced dipole forces. The electron density analysis of the NGBeO structures 1–3 reveals essentially charge-induced dipole interactions between the noble-gas atoms and BeO without any indication of covalent interaction. It cannot be excluded that attractive NG–Be interactions in 1–3 are partially enhanced by HOMO–LUMO interactions. However, all evidence points toward a classification of HeBeO , NeBeO , and ArBeO as unusually stable van der Waals complexes.

Acknowledgment. Part of this research has been supported by the National Science Foundation which provided computer time at the CRAY-XMP/48, San Diego Supercomputer Center (SDSC). We thank the staff of SDSC for excellent service and Dr. Mike Schmidt, North Dakota State University, for helpful discussions. Further support has been provided by the Deutsche Forschungsgemeinschaft, the Fonds der Chemischen Industrie, and the computer center of the Universität Köln.

Registry No. BeO , 1304-56-9; LiF , 7789-24-4; BN , 10043-11-5; LiH , 7580-67-8; He , 7440-59-7; Ne , 7440-01-9; Ar , 7440-37-1.

(56) Collins, J. R.; Frenking, G., to be published.

(57) (a) Yoshioka, Y.; Jordan, K. D. *J. Chem. Phys.* **1980**, *73*, 5899. (b) Yoshioka, Y.; Jordan, K. D. *Chem. Phys.* **1981**, *56*, 303.

Theoretical Investigation of the Ground and a Few Excited States of the Co(Schiff base)Li Complexes

Renato Colle,^{*,†} Alessandro Fortunelli,[‡] Nazzareno Re,[†] and Oriano Salvetti[‡]

Contribution from the Scuola Normale Superiore, Piazza dei Cavalieri, and Istituto di Chimica Quantistica ed Energetica Molecolare del CNR, Via Risorgimento 35, 56100 Pisa, Italy.

Received March 22, 1988

Abstract: RHF-plus-correlation calculations have been performed on the ground and a few excited states of the complex $\text{Co}(\text{foracim})_2\text{Li}$, chosen as a model of the $\text{Co}(\text{Schiff base})\text{Li}$ complexes. The wave functions thus obtained have been subjected to Mulliken population analysis and analyzed in terms of the orbitals of the separate constituent fragments to bring out effects of electronic σ -donation and π -back-donation between the cobalt atom and the ligand. The ground state of the isolated complex corresponds to an open-shell configuration of the $\text{Co}^{\text{II}}/\text{Li}$ type and of A_1 symmetry, with the triplet and singlet components practically degenerate. A permanent magnetic moment of the order of at least $1.9 \mu_B$ is predicted for the ground state of the complex. States corresponding to the configurations of the charge-transfer $\text{Co}^{\text{I}}/\text{Li}^+$ type are higher in energy by more than 1 eV.

The complexes of the transition-metal atoms with planar-tetradentate Schiff bases (SB), like acacen, salen, and salophen, are of much interest from both theoretical and experimental points of view.

Among the points of theoretical interest are the characterization of the particular effects related to the large numbers of electrons in these molecules, the analysis of the interaction between the d orbitals of the transition-metal atom and the delocalized π -system

of the organic ligand, and the prediction of their spectroscopic properties. However, only a limited number of theoretical studies of this type of molecule can be found in the literature.^{1–5} Few Hartree–Fock (HF) calculations are available, essentially because

(1) Sakaki, S.; Dedieu, A. *J. Organomet. Chem.* **1986**, *314*, C63.

(2) Di Bella, S.; Fragala, I.; Granozzi, G. *Inorg. Chem.* **1986**, *25*, 3997.

(3) Fisher-Hjalmars, I.; Henriksson-Enflo, A. *Adv. Quantum Chem.* **1982**, *16*, 1.

(4) Fantucci, P.; Valenti, V. *J. Am. Chem. Soc.* **1976**, *98*, 3833.

(5) Veillard, A.; Dedieu, A.; Rohmer, M. M. *J. Am. Chem. Soc.* **1976**, *98*, 5789.

[†] Scuola Normale Superiore.

[‡] Istituto di Chimica Quantistica ed Energetica Molecolare del CNR.